

# Sensor and Simulation Notes

Note 581

29 November 2018

## Study of Electromagnetic Field of a HEMP Simulator Located in a Wire Meshed Building

**Rakesh Kichouliya and Sandeep M Satav**  
Research Center Imarat, P.O. Vigyanakancha  
Hyderabad-500069, INDIA  
*Email: Rakesh.Kichouliya@rcilab.in*

### Abstract

An HEMP simulator is used to simulate the exo-atmospheric burst generated EMP as a plane wave field. In military standards this simulation is carried out by performing the RS105 test [1]. The HEMP simulator is a guided wave structure for generating an almost plane wave in the parallel plate section. This HEMP simulator has a lot of leakage fields distributed all around simulator. In some places, where space is constraint, the HEMP simulator is placed in the Faraday cage or in a shielded chamber, so that nearby electronic systems are not affected by its leakage fields. In this paper we have studied the effects of cage construction on the working volume fields inside the simulator, which may have significant effects on the equipment under test (EUT) due to late time response.

## 1. INTRODUCTION

High altitude nuclear electromagnetic pulse (HEMP) is generated as a byproduct of a nuclear detonation. The gamma rays from the nuclear detonation interact with air molecules through Compton process. This produces a transient electromagnetic field under the effect of earth's magnetic field[2]. The unclassified HEMP is defined in the IEC 61000-2-9 standard [3], which has a rise time of  $2.3 \pm 0.5$  ns and full width half maximum pulse width of  $23 \pm 5$  ns and peak electric field of 50 kV/m. The time domain and frequency domain characteristic is shown in Figures 1 and 2 respectively. There are mainly three types of HEMP simulators that have been developed and extensively used [4][5] to simulate the E1 pulse of HEMP. These are radiating type, conical or parallel plate transmission line type and hybrid type HEMP simulator. All three type of these simulators are required for qualifying an EUT for HEMP.

These simulators not only radiate the desired field in working volume, but also radiate the field all around the simulator[6][7]. These field may be quite high, depending upon the size and rating of the pulser and simulator. Typically these large simulators are established outdoors in a remote locations, where there are no nearby sensitive electronic systems[8]. But sometimes due to space constraints and smaller size, they are located inside a building, which may or may not have a wire mesh. Wire mesh is embedded in the walls of a building, where there are concerns of coupling effects to nearby critical electronic installations. By installing these wire meshes, all frequency components are confined within the building. The field is then reflected back towards the simulator and superimposed in the E field of the working volume. The reflected frequency components distort the field waveform in the working volume, whose effects may be additive or subtractive. The effects are important in testing object response at late time. In this paper we have studied an insitu HEMP facility in a wire mesh building, by using the Finite Integration Technique (FIT) technique[9] based code CST MW Studio 2015.0, and carried out its experimental verification.

## 2. HEMP SIMULATOR INSIDE THE BUILDING

The present HEMP simulator is a parallel plate type EMP simulator, located inside a wire mesh (2.5 cm x 2.5 cm, 2mm dia.) concrete building of 17m x 12m x 10m. The simulator is 8m long, 2m wide and 3m high. The simulator is excited by a 400 kV impulse generator, whose output is run through a peaking switch to generate the 50 kV/m field in the working volume. The simulator gives a rise time of 5 to 10 ns and pulse width of about 70 ns. The actual HEMP simulator is shown in Figure 3. The floor of the building has a copper ground plane. This simulator has been established inside a shielded building. This is primarily because there are many electronics labs located nearby, which may be affected by the leakage fields of this simulator. However by doing so the quality of the field waveform was compromised. The top view of simulator dimension in the building is shown in Figure 4.

## 3. HEMP SIMULATOR MODELING AND SIMULATION

To study the electromagnetic field of the HEMP simulator, a numerical model has been prepared and it is shown in Figure 5. In the model the simulator is excited by the double exponential voltage pulse having an amplitude of 1V, rise time of 5 ns, full width at half maximum pulse width of 30 ns. Total duration of the pulse is kept 400 ns to see the late time behaviour. The simulator is terminated with 150  $\Omega$  load resistance on the other side. The simulator is enclosed in a wire meshed (2.5 cm x 2.5 cm) building having dimension of 17 m (L) x 12 m (W) x 10 m (H). In the simulation thin wire model have been used for wire mesh. The concrete of the building walls is not considered in simulation, because for HEMP frequency range, the concrete does not exhibit dispersive properties. In the first step, the simulation was carried out and the field computed in the working volume. The fields were verified by measurements at the same point(0,3,1.5). The field measurement and simulation was done for dominant  $E_z$  component of the pulse, using the D dot sensor (Make Montena, Model no. SFE1G). The comparison of normalized simulation and measurement results is shown in Figure 6 and 7. It can be seen that late time reflections are seen in measured field inside the simulator.

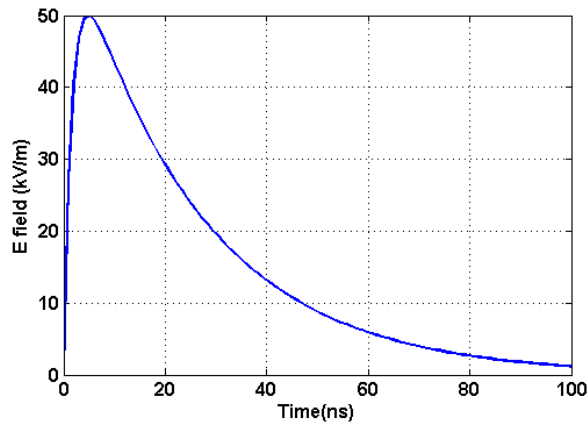


Figure 1. Time domain HEMP Waveform

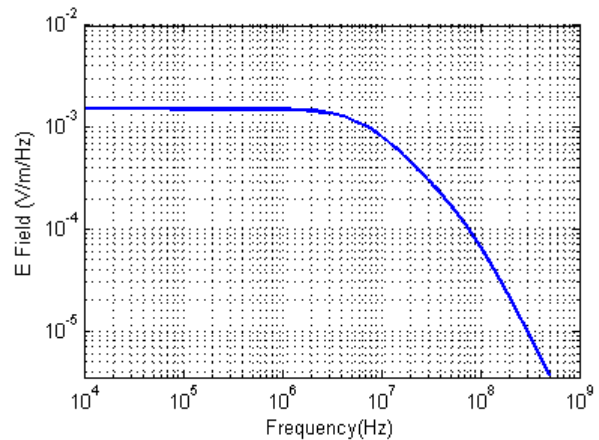


Figure 2. Frequency domain HEMP waveform

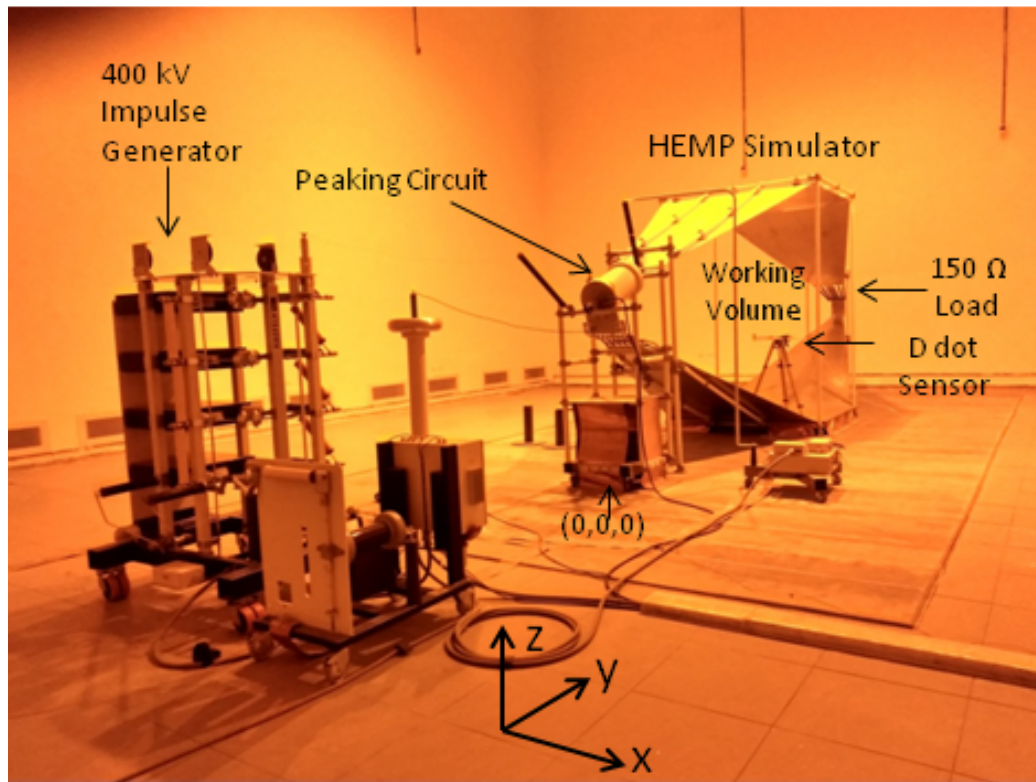


Figure 3. HEMP Simulator in wire caged building

### 3.1. HEMP field Simulation

The field simulation of the HEMP simulator has been carried out in three cases. In case-1, the simulation has been carried out in actual scenario i.e. simulator in wire mesh building. In case-2, the simulation is carried out with side wall mesh removed. In case-3, the simulation is carried out with wire mesh is completely removed. To study the effect of wire mesh on the field characteristics, four, 9 point grids, at 0.5 m, 1 m, 1.5 m and 2 m height have been chosen inside the working volume of the simulator. These grids are shown in Figure 8, 9 and 10. For case-1, Figure 8 shows the observation points, for case-2 Figure 9 shows the observation points and Figure 10 shows the observation points for case-3. The

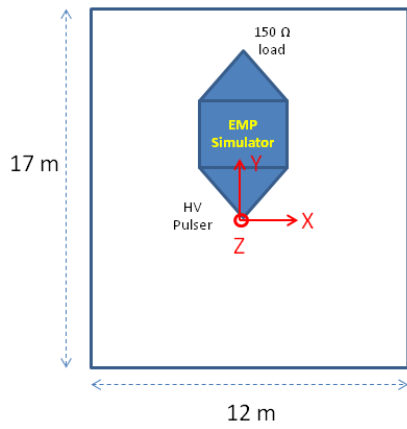


Figure 4. Top view simulator in building

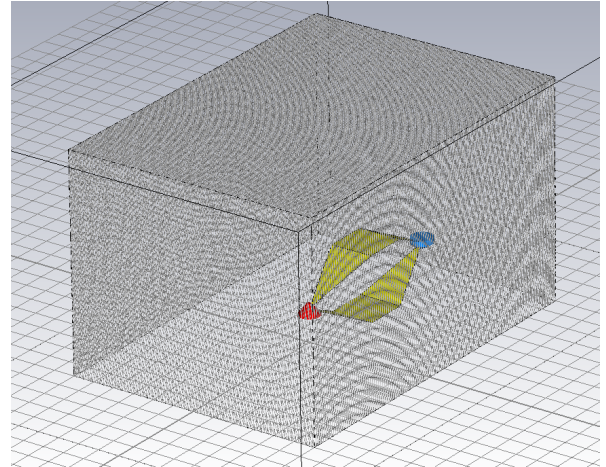


Figure 5. HEMP Simulator Model

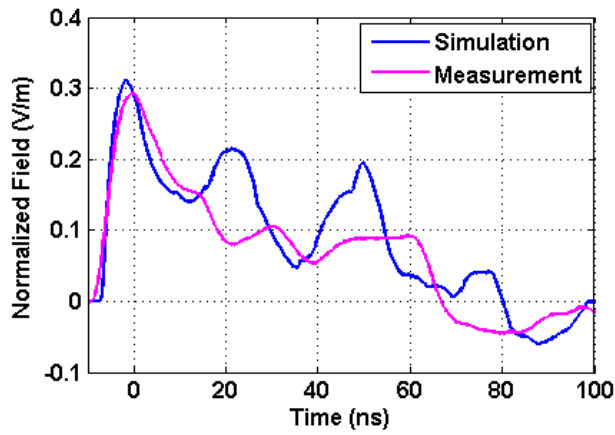


Figure 6. Validation of HEMP model

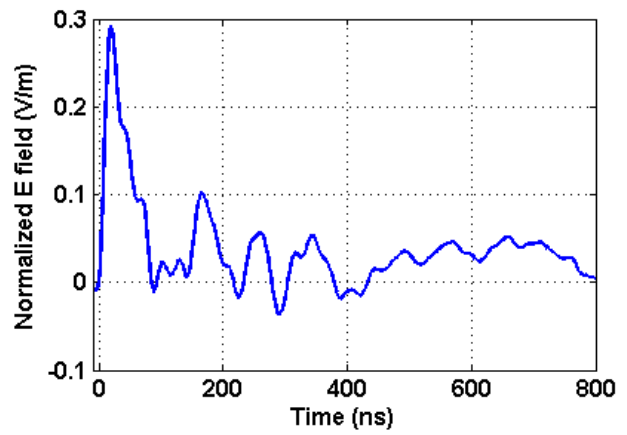


Figure 7. Measured E field at (0,3,1.5)

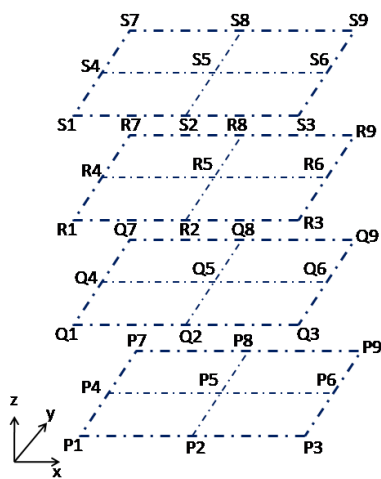


Figure 8. 9 point grid in working volume in case-1

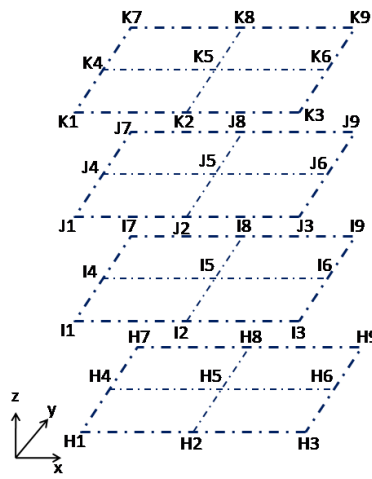


Figure 9. 9 point grid in working volume in case-2

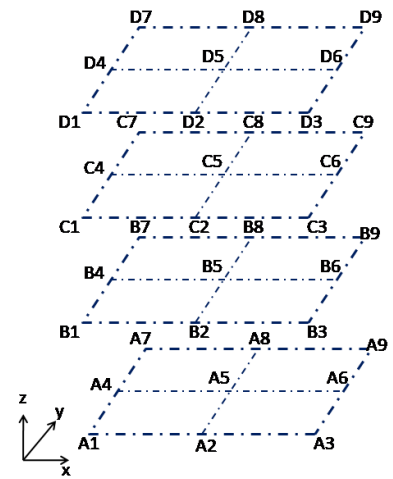


Figure 10. 9 point grid in working volume in case-3

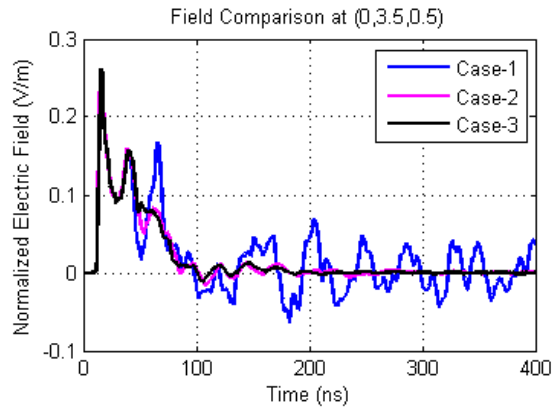


Figure 11. E field comparison at (0,3.5,0.5)

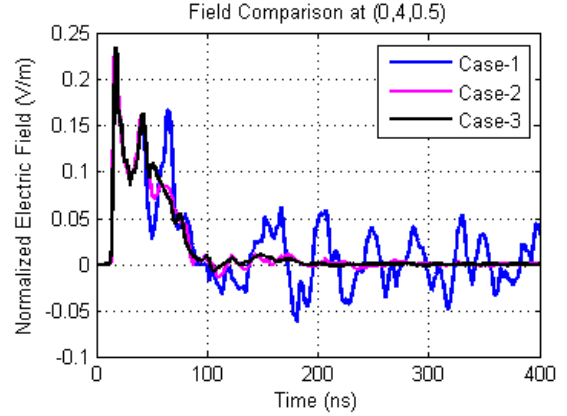


Figure 12. E field comparison at (0,4,0.5)

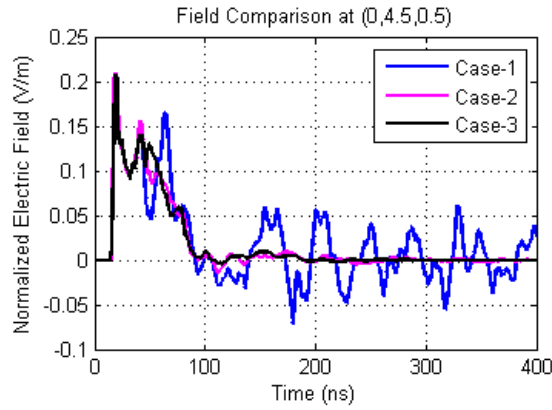


Figure 13. E field comparison at (0,4.5,0.5)

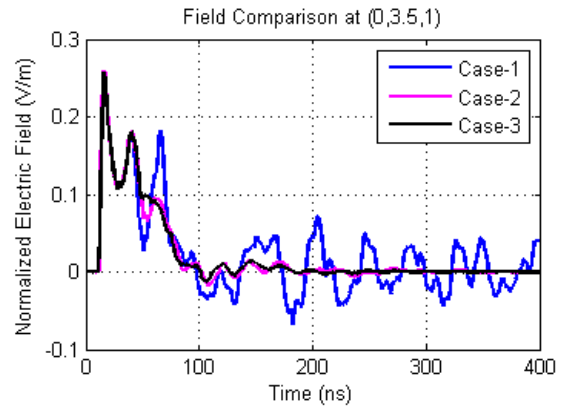


Figure 14. E field comparison at (0,3.5,1)

coordinate position for each point has been mentioned in table 1. The computed fields in all three cases are shown in Figure 11 to 22. The frequency domain fields are also computed and shown in Figure 23 to 34. The 2D surface plots are also shown in Figure 35 to 46 for  $z=1.5$  m along  $xy$  plane at the phase instant of 160 deg. at different frequencies.

Table 1. 9 Point grid position in case-1 (P,Q,R,S),case-2 (H,I,J,K) and case-3 (A,B,C,D)

| Sl. no. | Point Name | Co-ordinate Position |
|---------|------------|----------------------|------------|----------------------|------------|----------------------|------------|----------------------|
| 1       | P1,H1,A1   | (-0.5,3.5,0.5)       | Q1,I1,B1   | (-0.5,3.5,1)         | R1,J1,C1   | (-0.5,3.5,1.5)       | S1,K1,D1   | (-0.5,3.5,2)         |
| 2       | P2,H2,A2   | (0,3.5,0.5)          | Q2,I2,B2   | (0,3.5,1)            | R2,J2,C2   | (0,3.5,1.5)          | S2,K2,D2   | (0,3.5,2)            |
| 3       | P3,H3,A3   | (0.5,3.5,0.5)        | Q3,I3,B3   | (0.5,3.5,1)          | R3,J3,C3   | (0.5,3.5,1.5)        | S3,K3,D3   | (0.5,3.5,2)          |
| 4       | P4,H4,A4   | (-0.5,4,0.5)         | Q4,I4,B4   | (-0.5,4,1)           | R4,J4,C4   | (-0.5,4,1.5)         | S4,K4,D4   | (-0.5,4,2)           |
| 5       | P5,H5,A5   | (0,4,0.5)            | Q5,I5,B5   | (0,4,1)              | R5,J5,C5   | (0,4,1.5)            | S5,K5,D5   | (0,4,2)              |
| 6       | P6,H6,A6   | (0.5,4,0.5)          | Q6,I6,B6   | (0.5,4,1)            | R6,J6,C6   | (0.5,4,1.5)          | S6,K6,D6   | (0.5,4,2)            |
| 7       | P7,H7,A7   | (-0.5,4.5,0.5)       | Q7,I7,B7   | (-0.5,4.5,1)         | R7,J7,C7   | (-0.5,4.5,1.5)       | S7,K7,D7   | (-0.5,4.5,2)         |
| 8       | P8,H8,A8   | (0,4.5,0.5)          | Q8,I8,B8   | (0,4.5,1)            | R8,J8,C8   | (0,4.5,1.5)          | S8,K8,D8   | (0,4.5,2)            |
| 9       | P9,H9,A9   | (0.5,4.5,0.5)        | Q9,I9,B9   | (0.5,4.5,1)          | R9,J9,C9   | (0.5,4.5,1.5)        | S9,K9,D9   | (0.5,4.5,2)          |

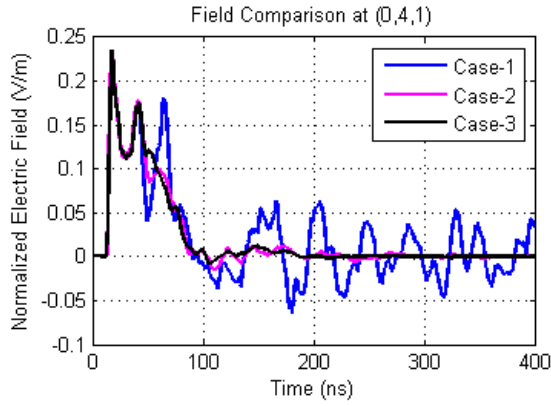


Figure 15. E field comparison at (0,4,1)

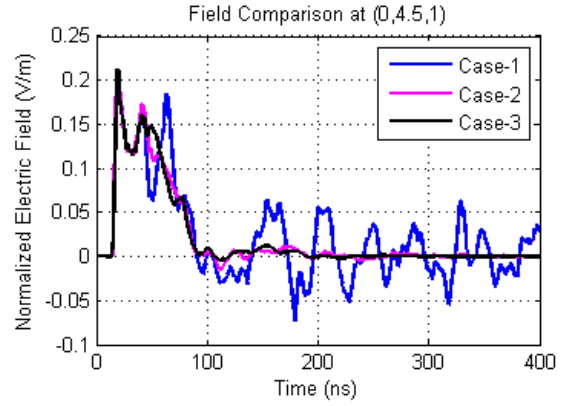


Figure 16. E field comparison at (0,4.5,1)

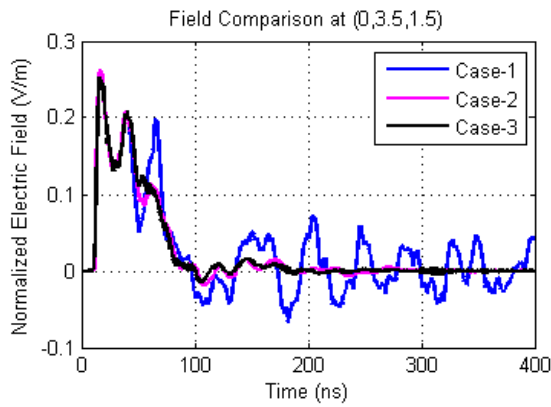


Figure 17. E field comparison at (0,3.5,1.5)

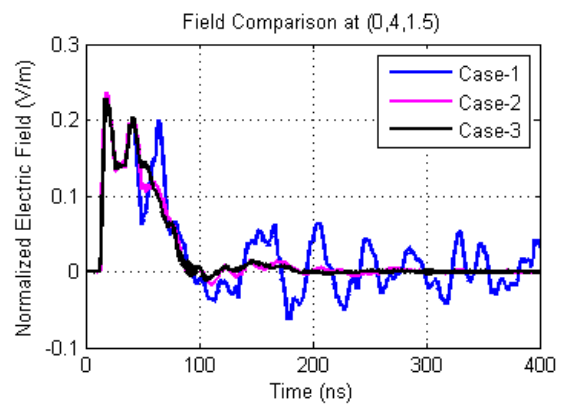


Figure 18. E field comparison at (0,4,1.5)

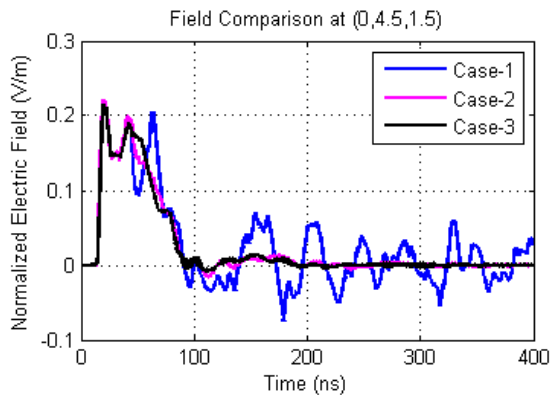


Figure 19. E field comparison at (0,4.5,1.5)

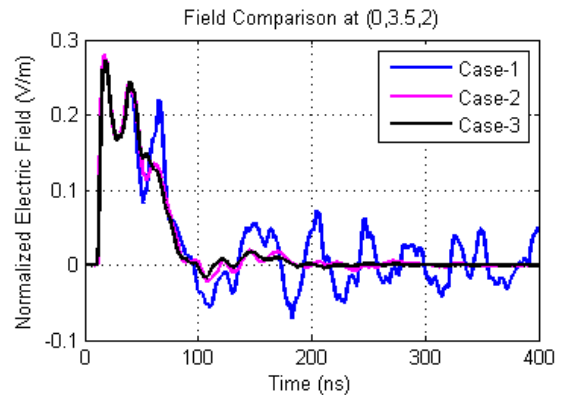
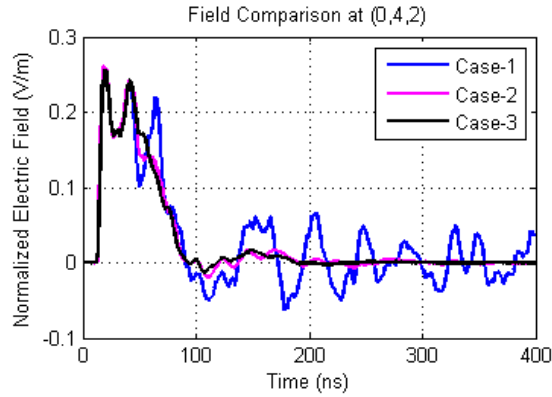
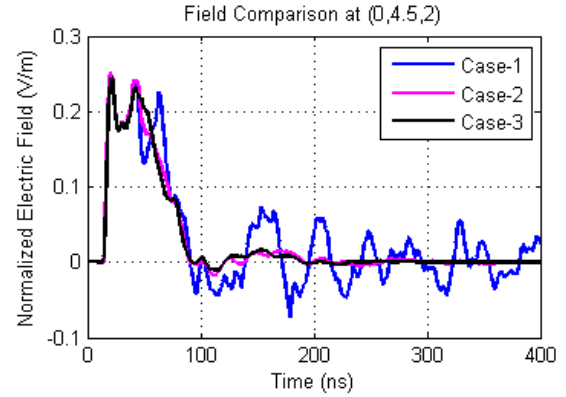


Figure 20. E field comparison at (0,3.5,2)



**Figure 21.** E field comparison at (0,4,2)



**Figure 22.** E field comparison at (0,4,5,2)

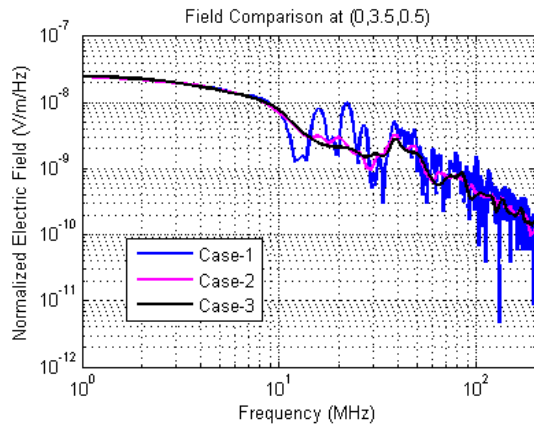


**Figure 23.** Frequency domain E field comparison at (0,3,5,0,5)

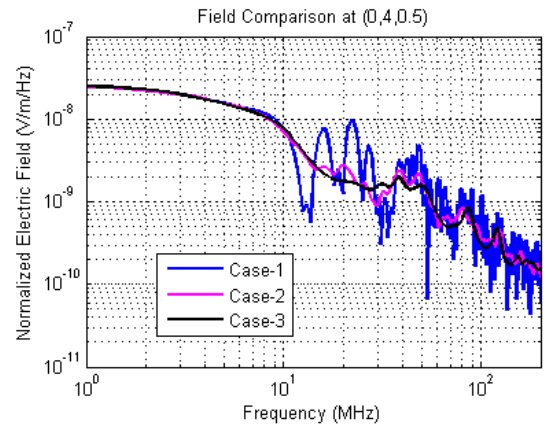


**Figure 24.** Frequency domain E field comparison at (0,4,0,5)

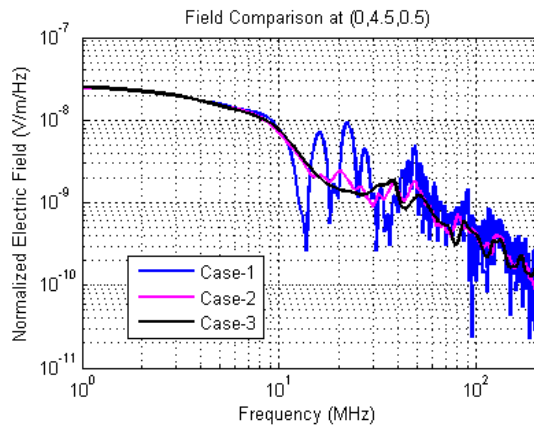


**Figure 25.** Frequency domain E field comparison at (0,4,5,0,5)

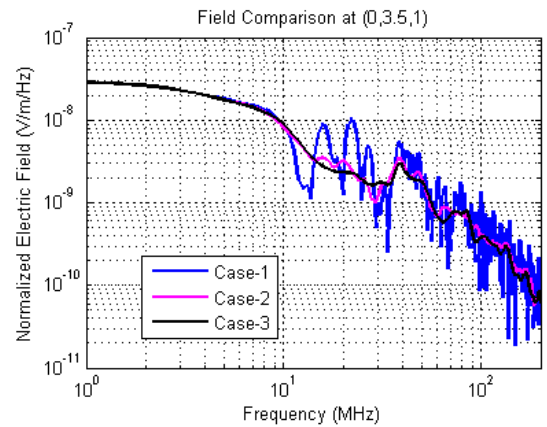


**Figure 26.** Frequency domain E field comparison at (0,3,5,1)

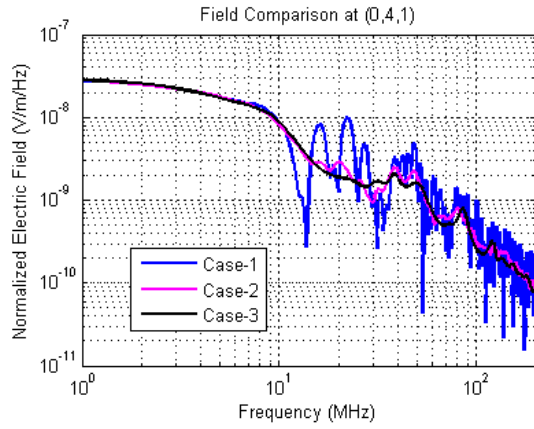


**Figure 27.** Frequency domain E field comparison at (0,4,1)

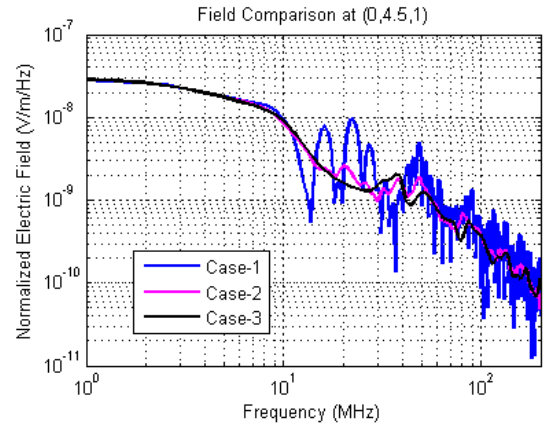


**Figure 28.** Frequency domain E field comparison at (0,4.5,1)

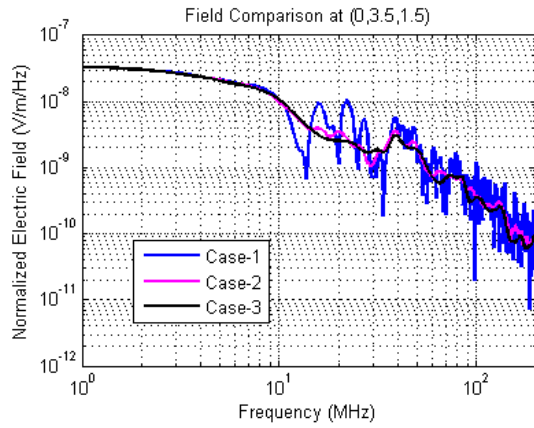


**Figure 29.** Frequency domain E field comparison at (0,3.5,1.5)

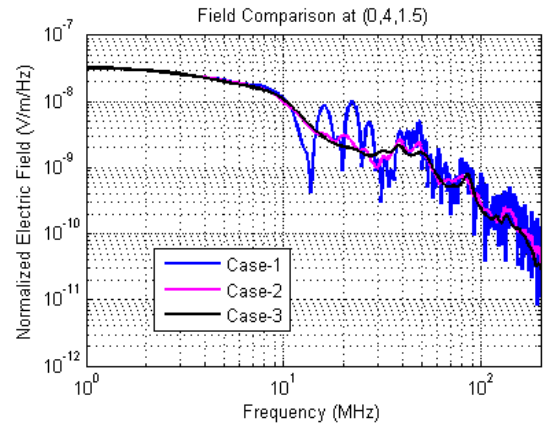


**Figure 30.** Frequency domain E field comparison at (0,4,1.5)

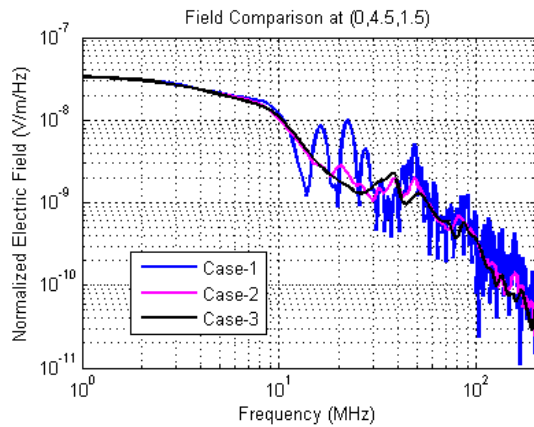


**Figure 31.** Frequency domain E field comparison at (0,4.5,1.5)

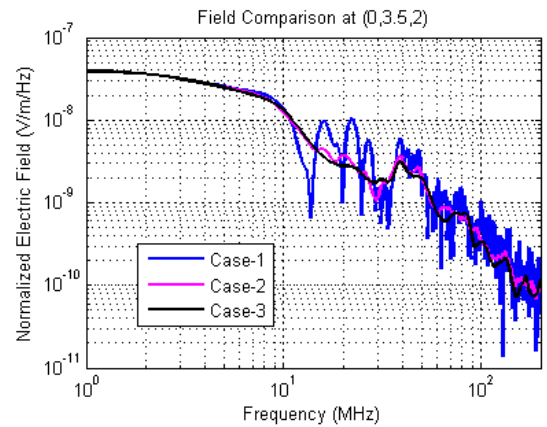


**Figure 32.** Frequency domain E field comparison at (0,3.5,2)

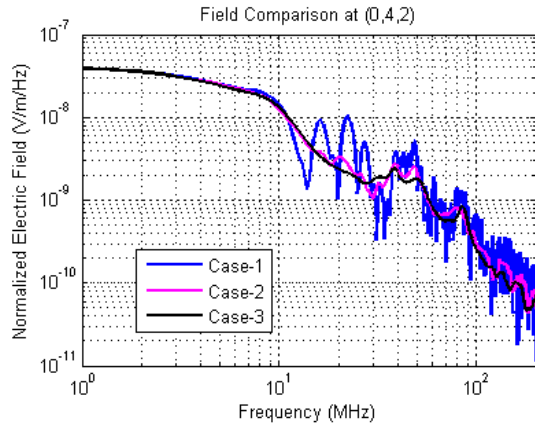


**Figure 33.** Frequency domain E field comparison at (0,4,2)

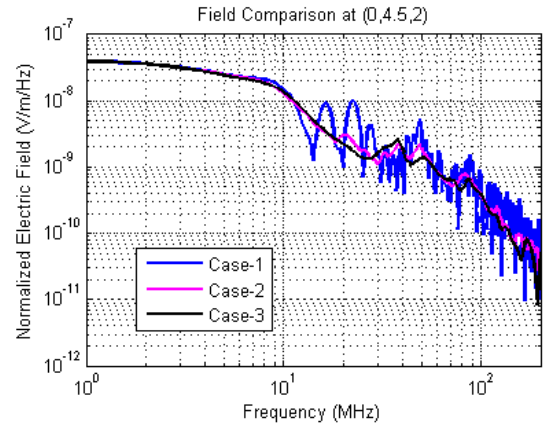


**Figure 34.** Frequency domain E field comparison at (0,4.5,2)

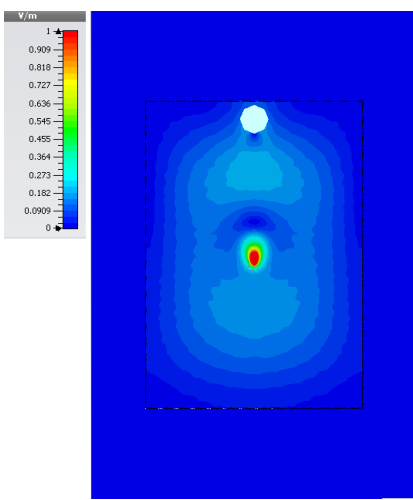


**Figure 35.** E field at 25 MHz in case-1

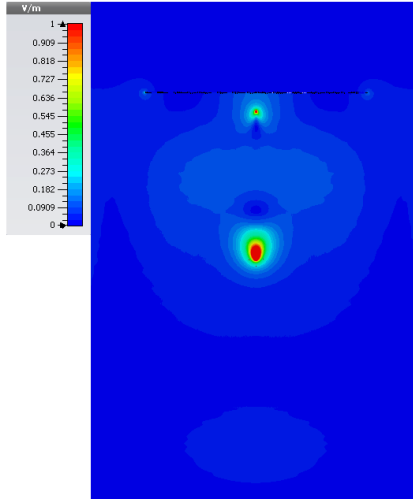


**Figure 36.** E field at 25 MHz in case-2

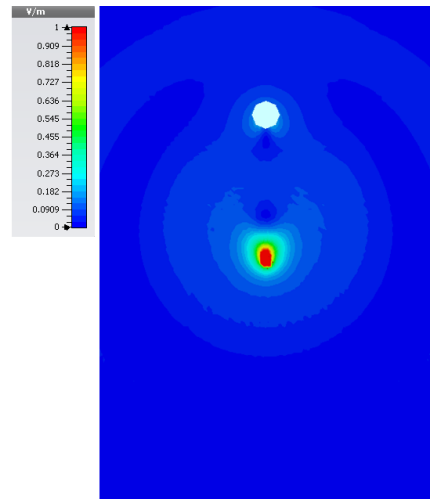


**Figure 37.** E field at 25 MHz in case-3

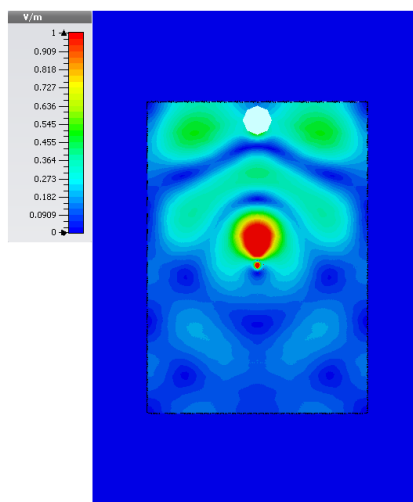


**Figure 38.** E field at 50 MHz in case-1

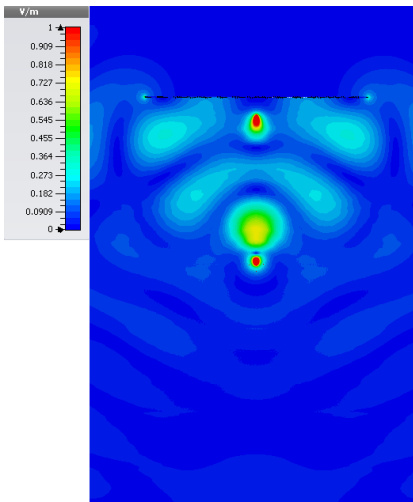


**Figure 39.** E field at 50 MHz in case-2

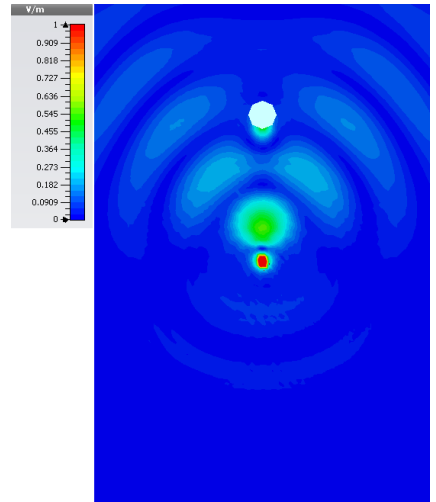


**Figure 40.** E field at 50 MHz in case-3

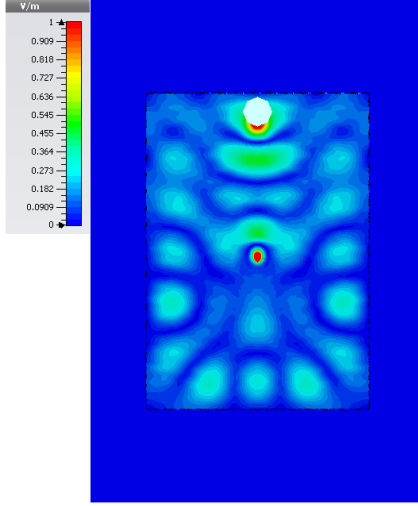


**Figure 41.** E field at 75 MHz in case-1

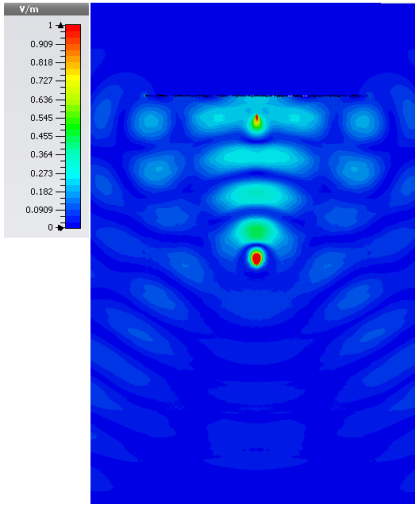


**Figure 42.** E field at 75 MHz in case-2

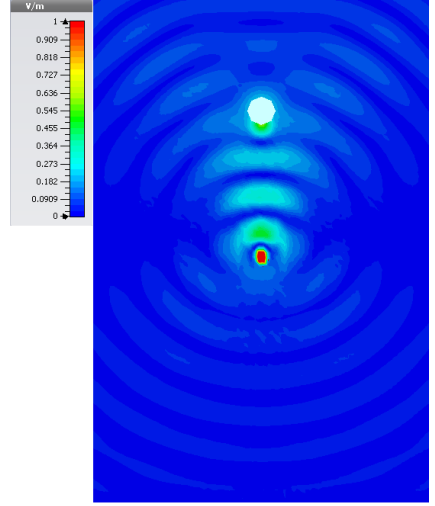


**Figure 43.** E field at 75 MHz in case-3

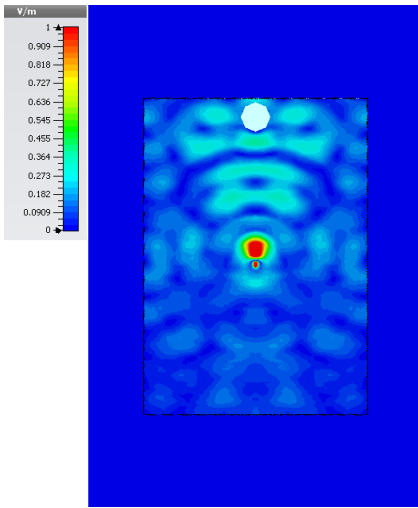


**Figure 44.** E field at 100 MHz in case-1

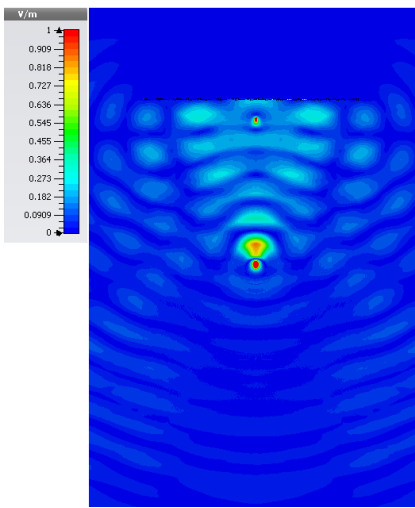


**Figure 45.** E field at 100 MHz in case-2

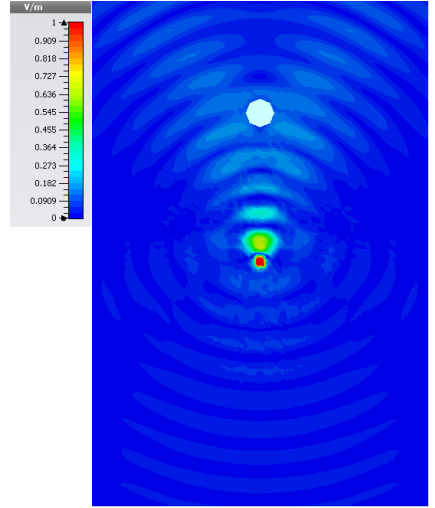


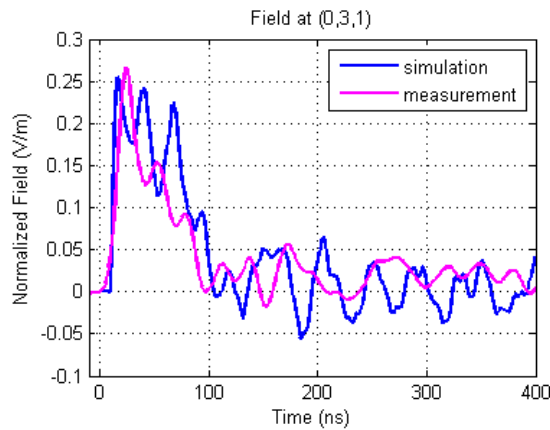
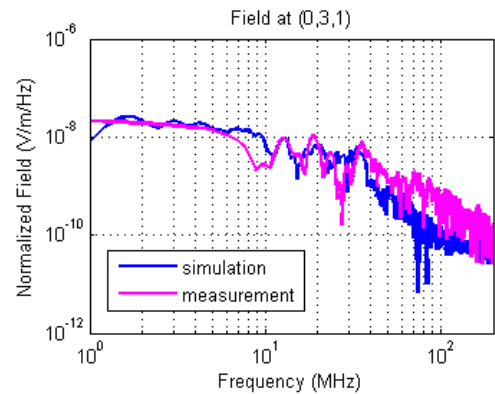
**Figure 46.** E field at 100 MHz in case-3

### 3.2. Computation of waveform norms

Waveform norms give important information about the characteristics of the waveforms, like energy content, rate of change of parameter and peak values etc[10]. The action integral is one such norm, which represents the energy content in the time domain waveform. The field in the working volume is found to have late time reflection in case-1 and almost no late time reflection in case-2 and case-3. The total energy content of the field in case-1 is expected to be higher than the other cases. Applying this norm to the electric field in the working volume of the HEMP simulator, where the wave impedance is close to  $377 \Omega$ , because of dominant TEM mode of propagation[10], the energy content of the field is computed at different location ( $x=0$ , YZ plane) in all three cases. The energy content of the fields is shown in table 2.

**Table 2.** Action Integral at various positions at  $x=0$ , in  $yz$  plane

| Sl. no. | Point Name | Normalized Action Integral in $377\Omega$ | Point Name | Normalized Action Integral in $377\Omega$ | Point Name | Normalized Action Integral in $377\Omega$ | Point Name | Normalized Action Integral in $377\Omega$ |
|---------|------------|---|------------|---|------------|---|------------|---|
| 1       | P2         | 0.003000                                  | Q2         | 0.003725                                  | R2         | 0.004782                                  | S2         | 0.006410                                  |
| 2       | P5         | 0.002927                                  | Q5         | 0.003490                                  | R5         | 0.004475                                  | S5         | 0.006120                                  |
| 3       | P8         | 0.002764                                  | Q8         | 0.003451                                  | R8         | 0.004516                                  | S8         | 0.006198                                  |
| 4       | H2         | 0.002246                                  | I2         | 0.002882                                  | J2         | 0.003841                                  | K2         | 0.005331                                  |
| 5       | H5         | 0.002142                                  | I5         | 0.002655                                  | J5         | 0.003565                                  | K5         | 0.005080                                  |
| 6       | H8         | 0.002007                                  | I8         | 0.002616                                  | J8         | 0.003598                                  | K8         | 0.005156                                  |
| 7       | A2         | 0.002199                                  | B2         | 0.002830                                  | C2         | 0.003776                                  | D2         | 0.005222                                  |
| 8       | A5         | 0.002110                                  | B5         | 0.002619                                  | C5         | 0.003508                                  | D5         | 0.004970                                  |
| 9       | A8         | 0.001999                                  | B8         | 0.002608                                  | C8         | 0.003565                                  | D8         | 0.005054                                  |

**Figure 47.** Time domain E field at  $(0,3,1)$ **Figure 48.** Frequency domain of E Field at  $(0,3,1)$ 

#### 4. HEMP SIMULATOR FIELD MEASUREMENTS INSIDE THE BUILDING

Field measurements in the working volume and outside of the HEMP simulator were also carried out at selected locations for case-1. A comparison is made with simulation results of case-1. The frequency domain field is computed by performing the Fourier transform of the simulated and measuring the time domain signal. The time domain and frequency domain fields at various locations are shown in Figures 47 to 58 for case-1. It can be seen that simulations and measurements results are closely matched.

#### 5. HEMP SIMULATOR FIELD SIMULATION AND MEASUREMENTS OUTSIDE THE BUILDING

The electric field was computed outside the shielded building in case-1 case-2 and case-3 at cartesian location  $(7,4,2)$ ,  $(0,-11,2)$ ,  $(0,10,2)$  and  $(0,8,12)$ . The fields were also measured at two points outside the building as shown in measurement set up in Figure 59. The computed field waveforms are shown in Figure 60 to 63 and they are compared with the measurement results at locations  $(7,4,2)$  and  $(0,10,2)$  in Figures 64 and 65 respectively.

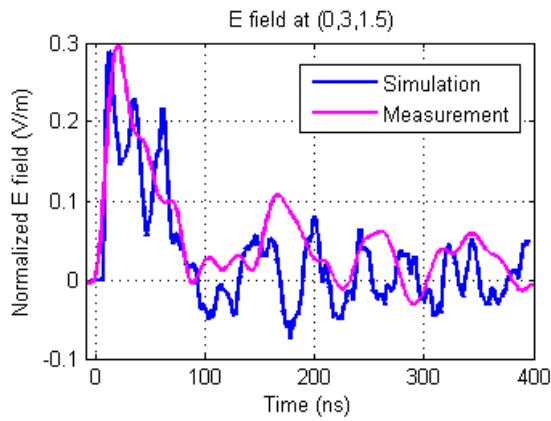


Figure 49. Time domain E field at (0,3,1.5)

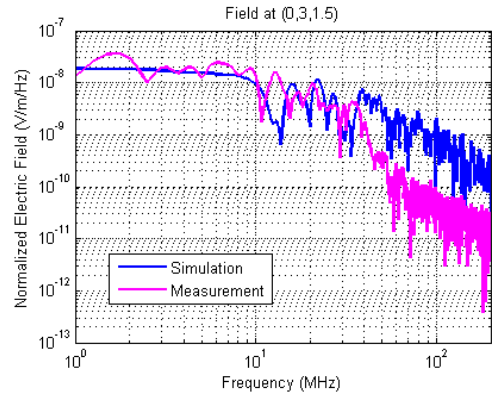


Figure 50. Frequency domain of E Field at (0,3,1.5)

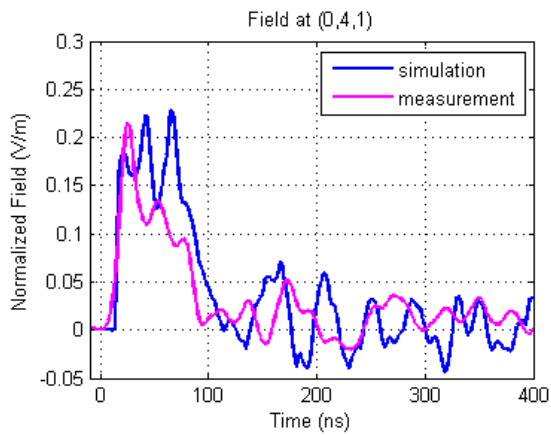


Figure 51. Time domain E field at (0,4,1)

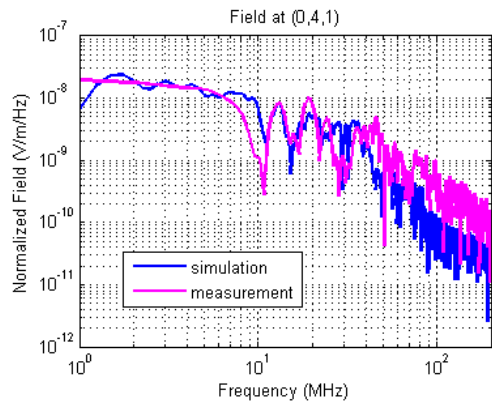


Figure 52. Frequency domain of E Field at (0,4,1)

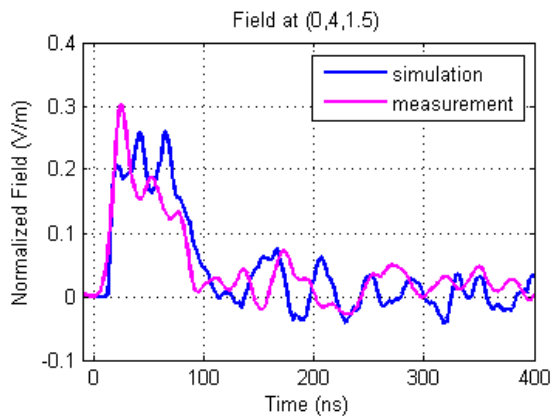


Figure 53. Time domain E field at (0,4,1.5)

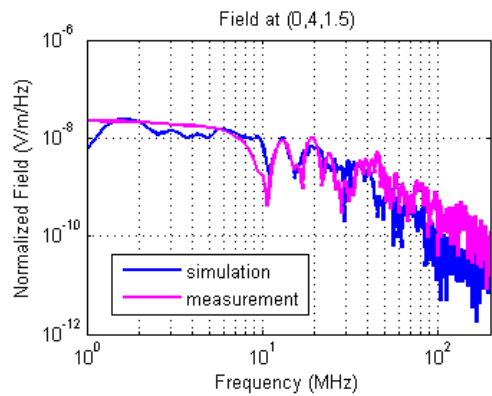


Figure 54. Frequency domain of E Field at (0,4,1.5)

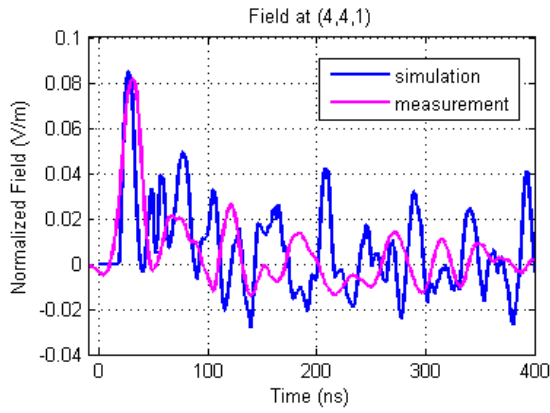


Figure 55. Time domain E field at (4,4,1)

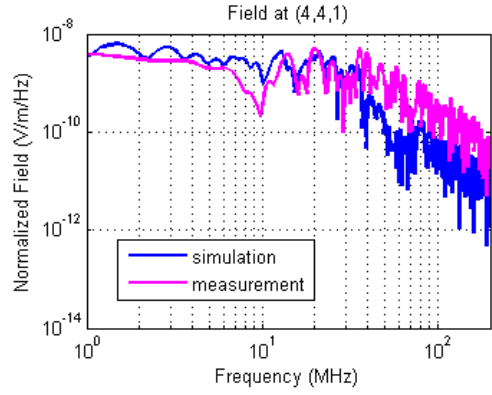


Figure 56. Frequency domain of E Field at (4,4,1)

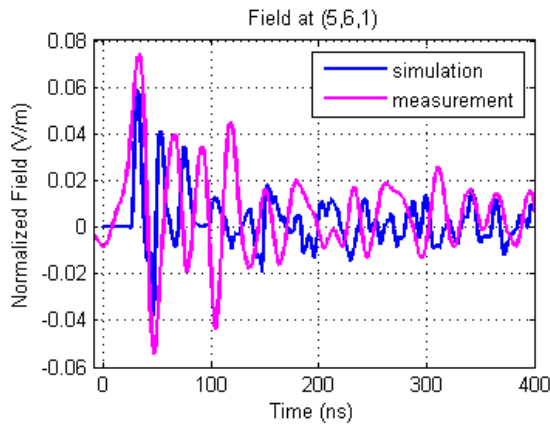


Figure 57. Time domain E field at (5,6,1)

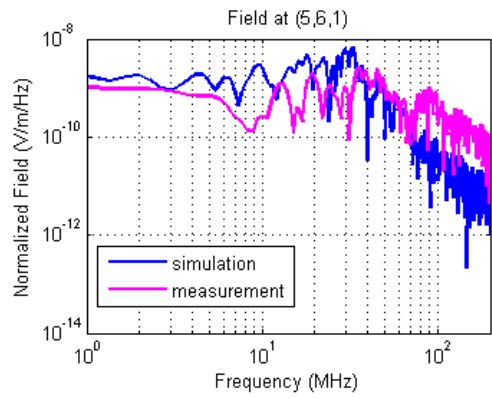


Figure 58. Frequency domain of E Field at (5,6,1)

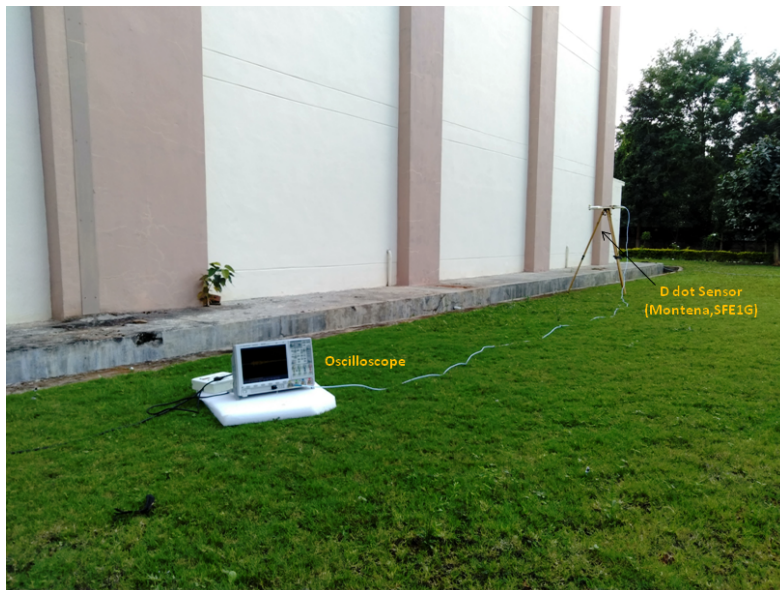


Figure 59. Field measurement outside building

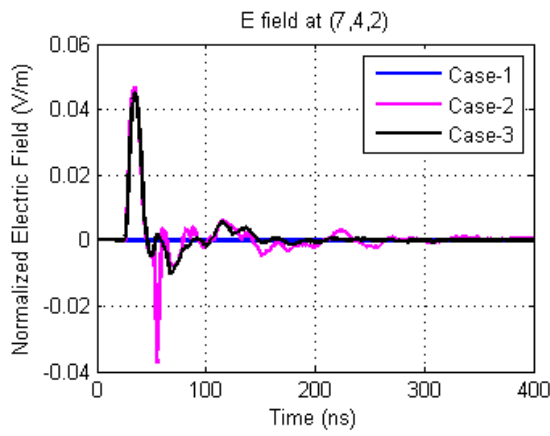


Figure 60. E field comparison at (7,4,2)

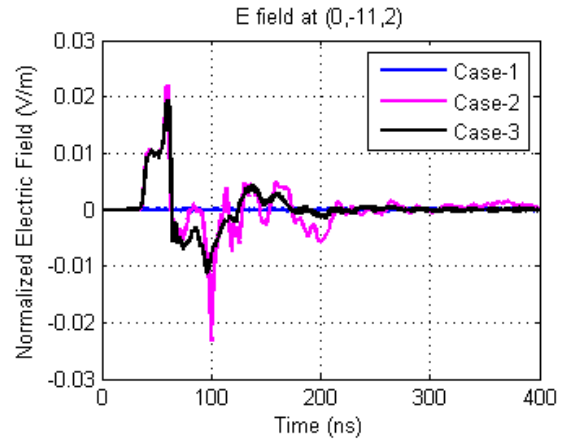


Figure 61. E field comparison at (0,-11,2)

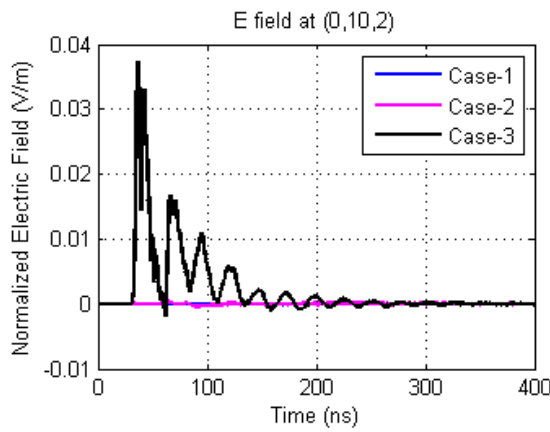


Figure 62. E field comparison at (0,10,2)

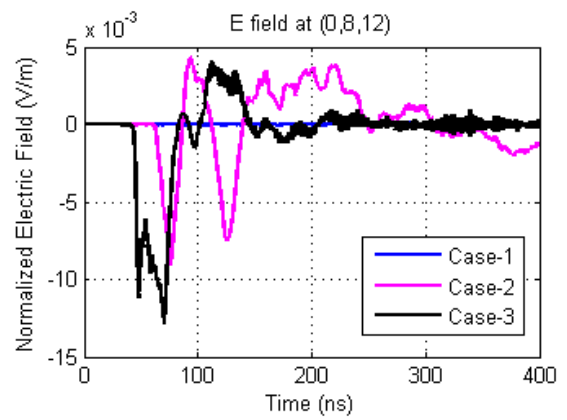


Figure 63. E field comparison at (0,8,12)

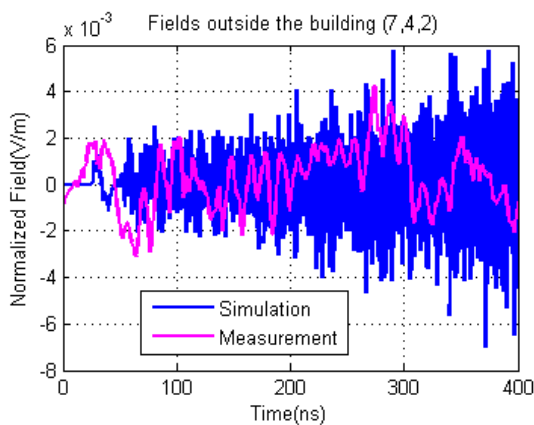


Figure 64. Comparison of E field at (7,4,2)

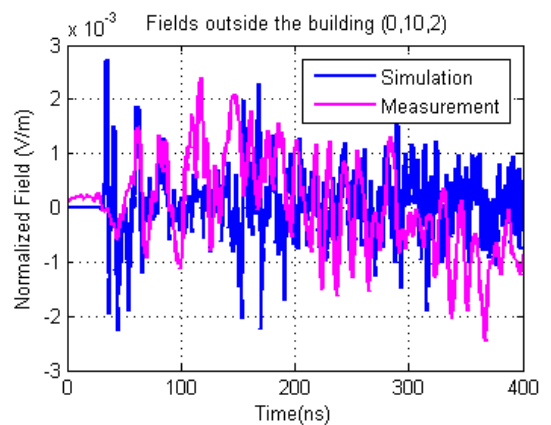


Figure 65. Comparison of E field at (0,10,2)

## 6. DISCUSSION ON RESULTS

The computed results in section 3 show that there are considerable reflections present in the late time of the E field pulse in the working volume of HEMP simulator. When the EMP simulator is operated, the E field travels in all directions. The wave gets reflected from wire-mesh locations and reaches to the measurement point. The total E field at measurement point is the sum of the E field in working volume and the reflected component from the wire mesh. The instant of reflection of the E field depends upon the round-trip distance travelled by the wave from the EMP simulator to the wall. It can be seen that in Figures 11 to 22, the first reflection from the side wall starts at 40 ns, which is exactly ( $12/3e8 = 40$  ns) the same. As the room dimension changes, the instant at which the reflection is seen also changes. If the room size is small the reflection will be seen in early time and if the room dimension is large the reflection will be seen in late time.

The high frequencies of the radiated field are confined to the forward direction within  $\pm 30deg.$  of the load end, middle frequencies propagate towards side walls and lower frequencies concentrate mainly back side of the simulator[12][13][14]. It can be seen from the frequency domain simulation and measurements plots from section 3 and 4, that the middle frequencies 10 MHz to 40 MHz has seen reflection in the amplitudes, while the frequencies above and below this band have smooth variation. The early reflections in the field (between 40 to 100 ns)and late time reflections are coming from the side wall of the wire-mesh buildings at middle frequencies of the pulse. At these frequencies the size of the mesh is small compared to the wavelength and it is acting almost as a short circuit. The late time reflections are caused by the surrounding shielded walls. It can be seen that the energy content of the field pulse in the working volume has been increased significantly in case-1, as compared to case-2 and case-3, due to the late time reflections. Also it can be observed from all the field plots, that by removing the side wall mesh in simulation of case-2 the late time reflections can be minimized. The removal of shielded mesh can be considered equivalent to putting RF absorbers/Ferrite in actual practice on side walls so as to minimize the reflections. There is minor effect seen on the working volume fields due to load end shielded wall. In case-3, which is free space simulation for the simulator, there is no such reflection seen in the simulator fields. The cavity effects are clearly visible from the 2D surface plots at various frequencies for case-1. The fields are creating a standing wave pattern inside the building. However, if the wire mesh wall is covered with RF absorbers/Ferrite, these effects can be minimized.

The action integral norm of the field waveform has been computed in the working volume. It can be seen that for the case-1 P,Q,R and S points the action integral is higher as compared to the the case-2 and case-3. This excess energy can cause the late time ringing response to EUT and it may be exposed to higher energy than desired. The field computation outside the shielded building was also carried out, and it can be seen that in case-1 there is almost negligible field present outside the building, while in case-2 and case-3 little field (leakage field ) is being radiated from HEMP simulator.

## 7. CONCLUSION

In this paper, the working volume field in the actual HEMP simulator has been studied. Late time reflections have been found in the fields, which are mainly due to side walls. These reflections may excite the late time responses to the EUT and may cause it to malfunction due to excess energy content. These reflections can be minimized by using RF absorber/ferrite tiles on side walls. Therefore it is concluded that an HEMP simulator should not be established in a shielded building, but if the circumstances demands so, than side walls must have the appropriate absorbing materials to damp out the late time reflections.

## ACKNOWLEDGMENT

The authors acknowledge the support and motivation from Director, RCI Hyderabad for conducting this study. The authors are grateful to engineers and staff of EMI-EMC Centre, RCI for assisting in

the the experimental work. The author's also acknowledges the motivation and guidance from Dr D. V. Giri in conducting this study.

## REFERENCES

1. "Department of Defence Interface Standard," Electromagnetic Environmental Effects Requirements for systems" *MIL-STD-464C*, 1 December, 2010.
2. R. Sherman, R. A. De Moss, W. C. Freeman, G.J. Greco, D.G. Larson, L. Levey, and D.S. Wilson, "EMP Engineering and Design Principles" *Bell Laboratories*, January 1975.
3. "Electromagnetic Compatibility, Part-2: Environment-Section-9: Description of HEMP Environment-Radiated Disturbance, Basic EMC Publication" *IEC 1000-2-9*, 1996-02, 38-40, 1996.
4. Carl E Baum., "EMP Simulators for Various Types of Nuclear EMP Environments: An Interim Categorization" *IEEE Transaction on Antennas and Propagation*, Vol. AP-26, No.1, January 1978.
5. Klassen J J A., "An Efficient Method for the Performance Analysis of Bounded-Wave Nuclear EMP Simulators" *IEEE Transaction on Electromagnetic Compatibility*, Vol.35, No.3, August 1993.
6. Frederick M. Tesche., "Prediction of E and H Fields Produced by the Swiss Mobile EMP Simulator (MEMPS)" *IEEE Transaction on Electromagnetic Compatibility*, Vol.34, No.4, November 1992.
7. Williams, W John et al., "Dipole Models for the Far-Field Representation of EMP Simulators with Application to Estimates of Human RF Exposure" *IEEE Transaction on Nuclear Science*, Vol.39, No.6, December 1992.
8. "Electromagnetic Compatibility, Part 4-32: Testing and Measurement Techniques-High Altitude Electromagnetic Pulse Simulator Compendium, Basic EMC Publication" *IEC 61000-4-32*, 2002-10, 2002.
9. Stephen D. Gedney, "Introduction to the Finite Difference Time Domain Method for Electromagnetics", Synthesis Lectures on Computational Electromagnetics, 2010.
10. Frederick M. Tesche., "CW Test Manual" *Measurement Note, Summa Foundation*, Note 64, 15 May 2013.
11. HAO-MING SHEN, RONALD W. P. KING and TAI TSUN WU., "The Exciting Mechanism of the Parallel Plate EMP Simulator" *IEEE Transaction on Electromagnetic Compatibility*, Vol. EMC-29, No.1, February 1987.
12. Carl E. Baum, D.V. Giri and Raymond D. Gonzalez, "Electromagnetic Field Distribution in TEM Mode in a symmetrical Two Parallel Plate Transmission Line" *Sensor and Simulation Notes 219, Summa Foundation*, SSN 219, 01 April 1976.
13. D. V. Giri, T.K.Liu, F. M. Tesche and R. W. P. King, "Parallel Plate Transmission Line Type of EMP Simulators: A Systematic Review and Recommendations" *Sensor and Simulation Notes 261, Summa Foundation*, SSN 261, 01 April 1980.
14. Kichouliya Rakesh et al., "Leakage Electric Field Analysis of a Guided Wave NEMP Simulator" *Proceedings of 2016 International Symposium on Electromagnetic Compatibility-EMC EUROPE 2016, Wroclaw, POLAND*, September 5-9, 2016.